POSSIBILITIES OFFERED BY MIG AND TIG BRAZING OF GALVANIZED ULTRA HIGH STRENGTH STEELS FOR AUTOMOTIVE APPLICATIONS

C. Chovet, S. Guiheux
Air Liquide / C.T.A.S. France

ABSTRACT

The subject of the study was to investigate the operating performances of braze welding technologies, particularly MIG-brazing and TIG-brazing, to join galvanized Ultra High Strength Steels, and to evaluate the metallurgical properties of the brazed joints.
In the experimental work done in CTAS a representative choice of steel grades and filler wires has been tested to assess their compatibility following several car manufacturers specifications. Tests were made on 1-2 mm thick plates and the grades DP 600 and TRIP 700 were chosen. The campaign of brazing trials was done with various copper wires. This evaluation comprises knowledge about the welding operation as well as the mechanical performances of the joints. Scanning electron microscopy has also been performed to characterize the bead and the copper / steel interface.
Our evaluation demonstrates that brazing with copper wires does not allow to reach similar mechanical properties than base materials due to the lower strength of the brazed metal. Nevertheless, the operating and mechanical results of MIG-brazing and TIG-brazing for ultra high strength steels sheets seems to be very promising because it should supply more reliable welding operating conditions on thin steel sheets.

KEYWORDS

Galvanized steels, Ultra High Strength Steels, braze welding, GTAW, GMAW, tensile-shear testing.

INTRODUCTION

The use of Ultra High Strength Steels (UHSS) in automotive industry is rapidly increasing since the end of the nineties. On recent car models they represent about 50% of the total mass of the body in white. The majority is Dual Phase steels with a tensile strength about 600 MPa. More and more applications of TRIP and Martensite steels with tensile strength up to 1500 MPa are reported. From a metallurgical point of view, a key issue of fusion welding of UHS steels is the tendency to create excessive hardness in the weld bead or in the heat affected zone which is very difficult to avoid. From the operating point of view, resistant spot welding process which is classically used in automotive industry is not well adapted to these UHSS because they require higher electrode forces and process modification to reduce hardness in weld metal [1]. The difficulty of arc welding on thin zinc coated sheets is to adapt the welding process for very thin sheets and to limit vaporization of the zinc layer which is detrimental for soundness of the welds and for in-service corrosion properties. Braze welding is an attractive alternative which allows to reduce drastically the heat input by about 50%.

1. EXPERIMENTAL PROCEDURE

1.1 BRAZE WELDING PROCESSES

Braze welding :
Braze welding is the process of joining metals whereby the melting temperature of the filler metal is above 450° C but below the melting point of the metals to be joined. It is very similar to fusion welding with the exception that the base metal is not melted. The filler metal is distributed onto the metal surfaces by tinning. Braze welding often produces bonds that are comparable to those made by fusion welding without the destruction of the base metal characteristics. Braze welding is also called bronze welding. Braze welding has many advantages over fusion welding. It allows to join dissimilar metals, to minimize heat distortion, and to reduce extensive pre-heating. Another side effect of braze welding is the elimination of residual stresses that are often present in fusion welding.

TIG (GTAW) process :
The process (Fig. 1) uses a non-consumable tungsten electrode to establish an arc transferring from a pointed tungsten electrode to the work piece in an inert atmosphere. The filler metal, when it is required, is fed into the arc with a cold or hot wire feed, which is independent of the heat input. The process mainly uses a constant current arc.

MIG/MAG (GMAW) process :
In the gas metal-arc welding process (GMAW), a consumable electrode (in the form of wire) is fed from a spool through the torch (welding gun) at a preset controlled speed. As the wire passes through the contact tube of the gun, it picks up the welding current. The consumable wire electrode serves two functions: it maintains the arc and provides filler metal to the joint. The weld metal is shielded from the atmosphere by a flow of an inert gas (MIG), or an active gas (MAG). Fig. 2 illustrates this process.

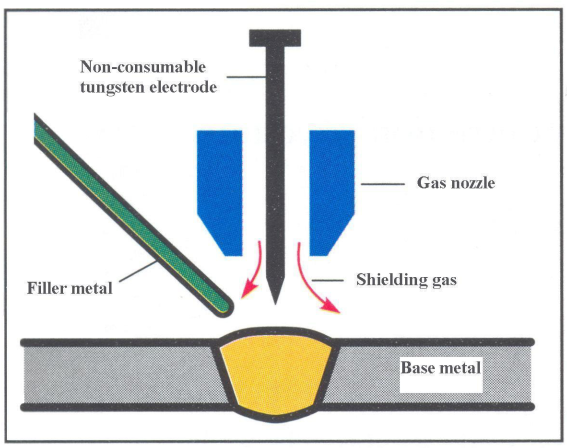

Fig. 1 : TIG process operation

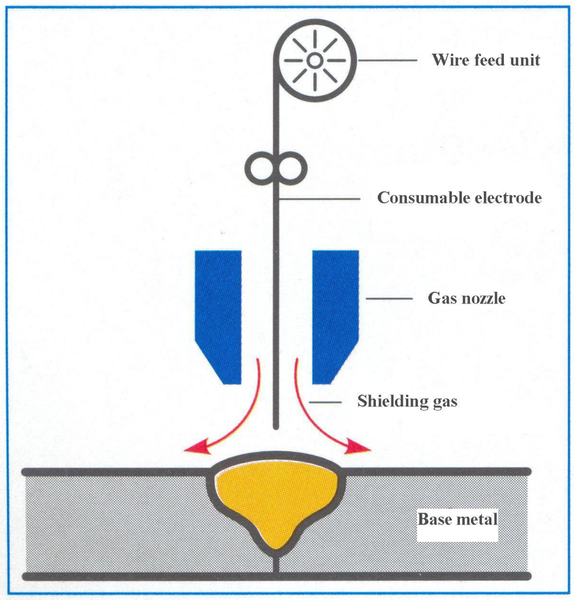

Fig. 2 : MIG process operation

1.2 MATERIALS AND CONSUMABLES

After an evaluation in research programs and on prototypes, car makers include more and more of UHSS on high volume car models [2]. According to the ULSAB-AVC Program [3], sponsored by a consortium of about 35 international steel producers, and to the New Car Steel Body concept of THYSSEN, more than 70% of the body structure can be composed of UHSS.

The motivation for the use of UHSS for car manufacturing is essentially seen in two reasons : weight reduction and crash performances. In fact, these UHSS exhibit superior combination of high strength and good formability. This combination arises primarily from their high strain hardening capacity as a result of their lower yield strength to ultimate tensile strength ratio 4. These UHSS are produced by controlling the cooling rate from the austenite or austenite plus ferrite phase, either on the runout table of hot mill or in the cooling section of a continuous annealing furnace. The UHSS used in automotive industry are mainly Dual Phase and TRIP steels. The microstructure of dual phase steels is comprised of soft ferrite and between 20 and 70% volume fraction of hard phases (martensite and/or bainite). The DP sheet steel are made ductile by the soft ferrite phase and their strength is controlled by the amount of martensite. So that DP steels have a much higher ultimate tensile strength than conventional steels of similar yield strength. The properties of the steel can be controlled in accordance with the amount of martensite. The microstructure of TRIP steels consists of a continuous ferrite matrix containing a dispersion of hard second phases (martensite and/or bainite) and also a retained austenite volume fraction greater than 5%. During deformation, the dispersion of hard second phases in soft ferrite creates a high work hardening rate, as in DP steels. However, in TRIP steels, the retained austenite progressively transforms to martensite with increasing strain, thereby increasing the work hardening rate.

For the experimentation, a Dual Phase DP600 and a TRIP 700 steel were chosen. The chemical composition and properties are given in Table 1 and Table 2.

Table 1 : Properties of DP600 and TRIP700 steels

Grades	DP 600	TRIP 700
Micrograph	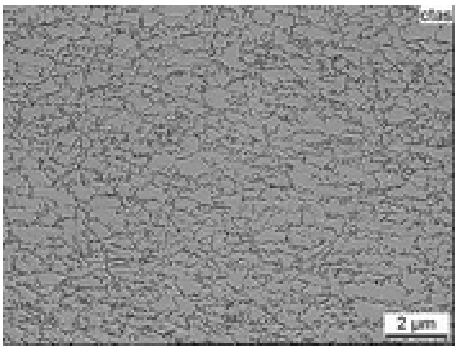	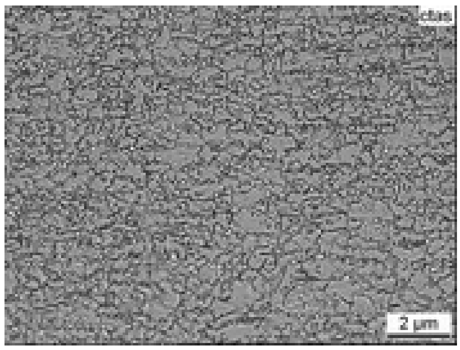
Microstructure	Mainly ferritic with a fraction of hard phases (martensite) Retained austenite : ~ 5%	Mainly ferritic with a higher fraction of hard phases (martensite) Retained austenite : ~ 15%
Coating	Zn thickness : 12/13 µm	Zn thickness : 12/13 µm
Mechanical properties	Rp0.2 = 382 MPa Rm = 607 MPa A% = 30 %	Rp0.2 = 451 MPa Rm = 680 MPa A% = 36 %

HOME

Table 2 : Chemical composition of DP600 and TRIP700

Material Type	Grades	Chemical composition							
		C	Mn	Si	Al	Ti	B	S	P
Dual Phase	DP 600	0.122	1.460	0.055	1.270	0.006	0.0003	0.0010	0.013
Transformation Induced Plasticity	TRIP 700	0.225	1.750	0.052	1.550	0.006	0.0006	0.0010	0.014

Table 3 : Filler wires used for braze welding trials

Wire	Type	Supplier	ϕ (mm)	Rm* (MPa)	Chemical composition			
					Al	Mn	Ni	Fe
Solid wires								
Nertalic 46	CuAl8	AIR LIQUIDE WELDING	1.2	420	8.5	1.8		
AlBz35	CuAlNi6	BEDRA	1.2	690	9	1.5	5	3.5
Maxal 300	CuMn13Al7	BEDRA	1.2	900	8	13	2.5	2.5
Flux cored wire								
Mecufil 214 Al		STEIN	1		13.4			

** tensile strength obtained on all-weld-metal deposit*

Braze welding trials were done with one copper solid wire supplied by AIR LIQUIDE WELDING for braze welding of galvanized sheets, two copper solid wires supplied by BEDRA as standard product mainly for hard surfacing applications and one copper flux cored wire supplied by STEIN for this application precisely. An analysis of these wires is given in the Table 3. The solid wires CuAlNi6 and CuMn13Al7 were chosen according to their tensile strength in order to match mechanical properties of base metals.

1.3 BRAZE WELDING PARAMETERS

The majority of welds on body-in-white is done in lap joint configuration without backing plate (without forced thermal discharge) [5] [6]. During this study, the assemblies were welded in lap joint configuration as shown in Fig. 3, without any gap between the sheet. Note that in real production the gap might be one time the sheet thickness. For MIG braze welding, the wire impact was adjusted exactly in the angle of the lap joint with a forehand travel angle of about 20° and a working angle of 20° (see Fig. 3).

All braze welding tests were performed automatically on a machine or a robot. TIG braze welding was done with the new TOPTIG torch [7] from AIR LIQUIDE WELDING which allows higher welding speed than conventional TIG torch. For MIG braze welding the shielding gas used was pure Argon, whereas for TIG braze welding we used ARCAL 10 gas, which is a mixture of Argon and Hydrogen. Indeed, Hydrogen addition improves the quality of the bead appearance. The wire feed speed WFS was chosen to obtain a sufficient joint section and depends on wire diameter, welding speed and sheet thickness. Welding speed was mainly ws=60cm/min for MIG braze welding and between 45 and 120 cm/min for TIG braze welding. Braze welding parameters are shown in Table 4. Note that for MIG braze welding, a short arc transfer was used and for TIG braze welding, direct current was used.

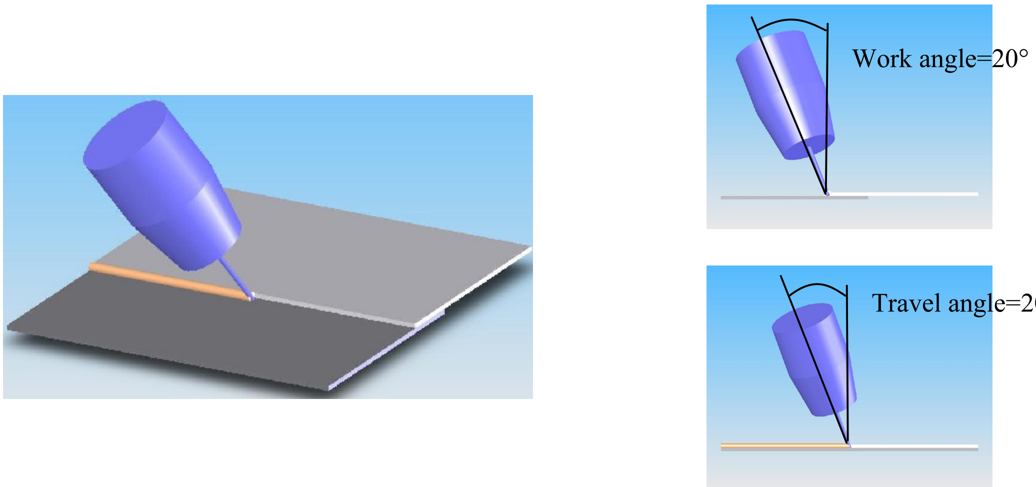

Fig. 3 : Lap joint and impact of wire for MIG process

Table 4 : Braze welding parameters

MIG brazed joints										
Gaz	**Chemistry**	**∅**	**Sheet**	**e**	**WS**	**WFS**	**U**	**I**	**E lin**	**E lin norm**
		mm		**mm**	**m/min**	**cm/min**	**V**	**A**	**J/cm**	**J/cm/mm**
Arcal 1	CuAlNi6	1.2	DP 600	1	3	60	12.8	103.0	1318.4	1318.4
			TRIP 700	2	5	60	13.6	159.0	2162.4	1081.2
	CuMn13Al7	1.2	DP 600	1	3	60	14.3	82.0	1172.6	1172.6
			TRIP 700	2	5	60	15.4	133.0	2048.2	1024.1
	CuAl8	1.2	DP 600	1	4	60	14.2	95.1	1349.2	1349.2
			TRIP 700	1	4	60	14.9	85.9	1281.9	1281.9
	Mecufil 214	1	DP 600	1	4	60	12.8	90.1	1148.1	1148.1
			TRIP 700	1	4	60	15.2	77.1	1173.5	1173.5

TIG Brazed joints										
Gaz	**Chemistry**	**∅**	**Sheet**	**e**	**WS**	**WFS**	**U**	**I**	**E lin**	**E lin norm**
		mm		**mm**	**m/min**	**cm/min**	**V**	**A**	**J/cm**	**J/cm/mm**
Arcal 10	CuAlNi6	1.2	TRIP 700	2	4.7	80	14.0	200.0	2100.0	1050.0
	CuMn13Al7	1.2	TRIP 700	2	4.8	120	14.5	200.0	1450.0	725.0
	CuAl8	1.2	DP 600	1	2.45	45	12.0	100.0	1600.0	1600.0
			TRIP 700	1	2.8	50	12.0	100.0	1440.0	1440.0

In order to compare the results, the heat input has been normalized over the sheet thickness and an efficiency coefficient depending on the weld process :

$$E_{linear} = \frac{U * I}{WS} * 60 * \eta \qquad (1)$$

$$E_{normalized} = \frac{E_{linear}}{e} \qquad (2)$$

where : U : voltage (V), I : current (A), e : thickness (mm), WS : welding speed (cm/min) and η : process coefficient ($\eta_{TIG} = 0.5$ and $\eta_{MIG} = 0.7$).

1.4. CHARACTERIZATION OF THE JOINTS

Macrographic sections of the joints were cut transverse to the travel direction. They were mechanically polished, then etched with Nital (4% HNO_3 in water). Macrographs and micrographs were realized under light optical microscopy.

Lap joints were mechanically characterized by tensile-shear testing. Shape and dimension of tensile-shear specimens are shown on Fig. 4. With this kind of test, tensile stress as well as shear stress are applied to the joints. Tensile-shear specimens were cut from 230 mm long welds, thus avoiding the presence of arc start and arc extinction is the relevant zone. The bead surface was not machined prior to testing. Three specimens per joints have been realized. For this test, the tensile strength Rm has been defined as the ratio between the maximum force and the section taking into account one sheet thickness (for example, for a lap joint of 1 mm thick sheets, the section would be 20x1 mm^2).

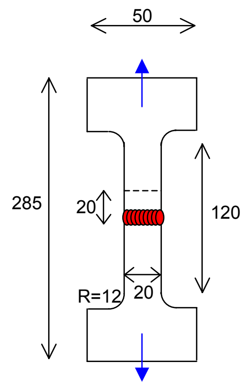

Fig. 4 : design of tensile test specimen

2. BRAZE WELDING RESULTS

2.1. METALLOGRAPHIC EXAMINATION

Visual aspects of the beads for the two braze welding processes are shown on Fig. 5. Both examples were brazed with CuAl8 wire. Compared to MAG welding which often leads to porosities in the weld bead due to zinc vaporization, weld brazing gives sound beads. One can notice a smoother bead aspect with TIG braze welding. Only a few spatters are given by MIG braze welding, whereas TIG process lead to almost no spatters.

Representative cross sections are shown on Fig. 6. No particular differences have been observed concerning the weld bead shape and the appearance with varying base metal and filler wires. Examples shown are cross sections of beads obtained CuAl8 wire for both processes and both steel grades. In all cases, the dilution of the bottom sheet is low. The dilution of the top sheet can be a little higher. Compared to MAG welding, the low heat input of these processes leads to a more reliable joining of thin sheets, due to a lower risk of burn through. One can also observe a good wetting angle, largely superior to 90° as specify by car makers ([5] and [8]). A penetration of the copper in the gap between the two sheets is appreciated for better mechanical resistance which is the case on the cross sections showed.

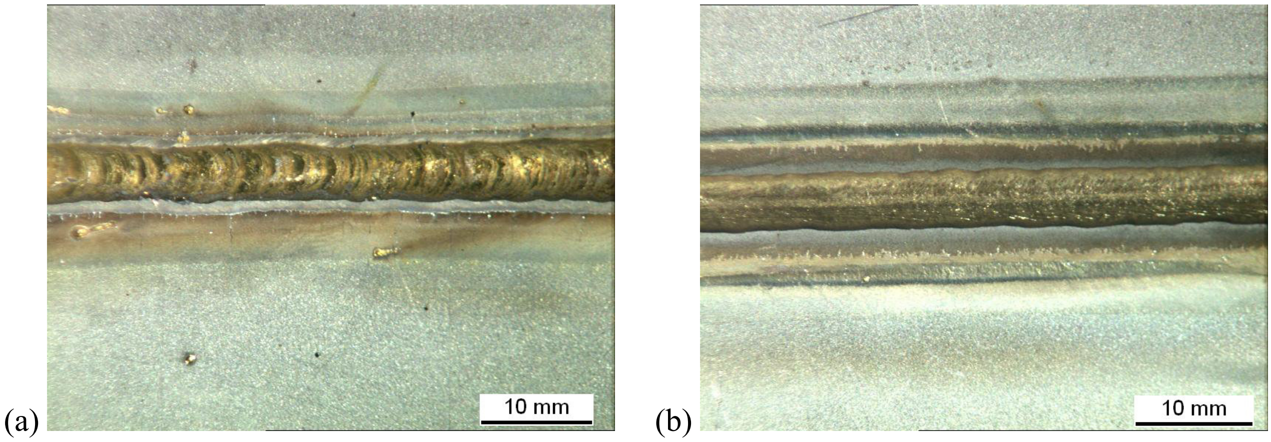

Fig. 5 : visual aspect of beads obtained for (a) MIG braze welding on TRIP 700 with Nertalic 46 wire and (b) TIG braze welding on DP 600 with Nertalic 46 wire.

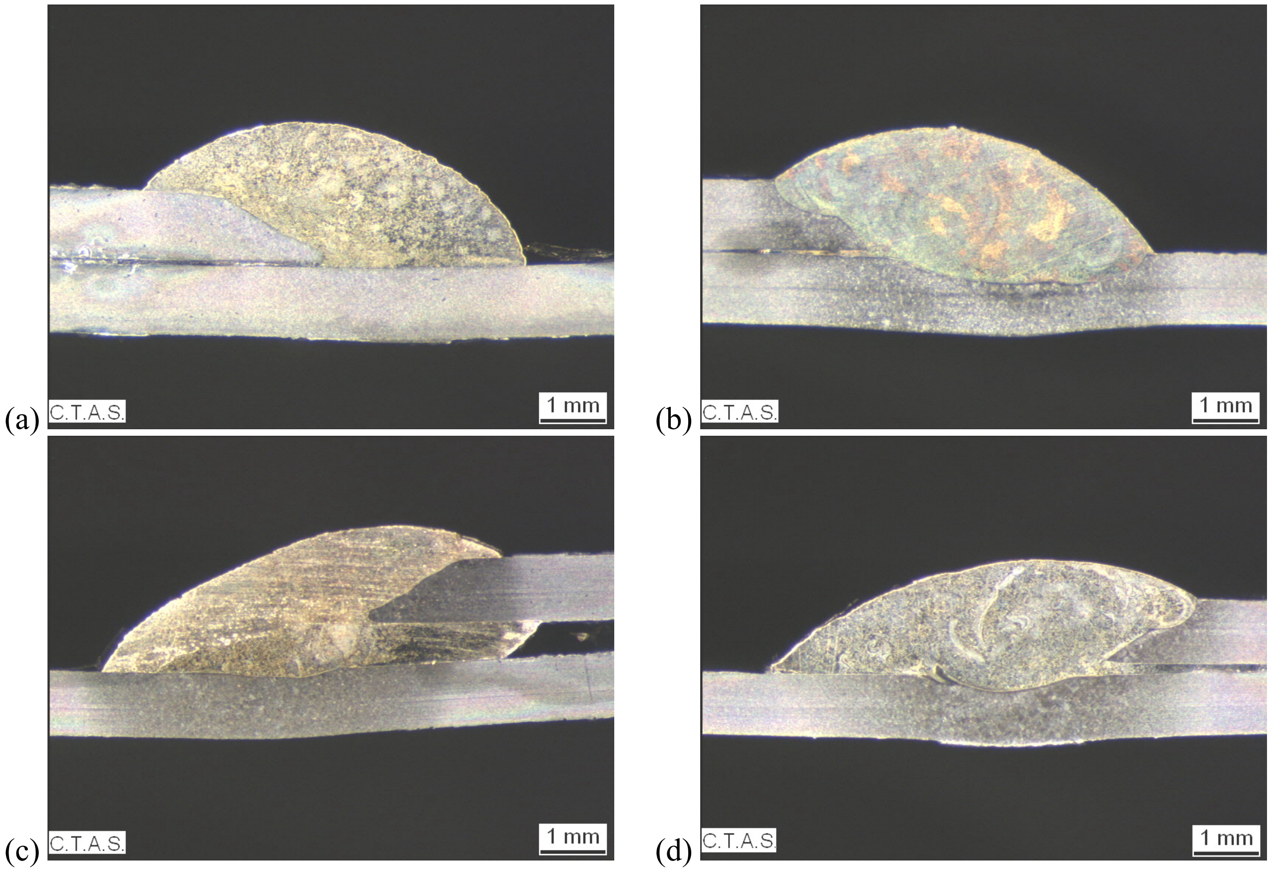

Fig. 6 : cross sections obtained with $CuAl_8$ wire of (a) MIG brazed joint on DP600, (b) TIG brazed joint on DP600, (c) MIG brazed joint on TRIP700, (d) TIG brazed joint on TRIP700.

Examples of micrographs of beads obtained in MIG braze welding with the various filler wires are presented in Fig. 7. In all cases, the bead is composed of a copper matrix with iron, coming from the low dilution of the base metal. Iron in the copper matrix can be either in the shape of dendrites or in the shape of spherical inclusions. SEM investigations showed that dendrite shape forms for higher iron concentration than spherical shape inclusions. Then, the higher the dilution is, the more dendrite are found in the copper matrix.

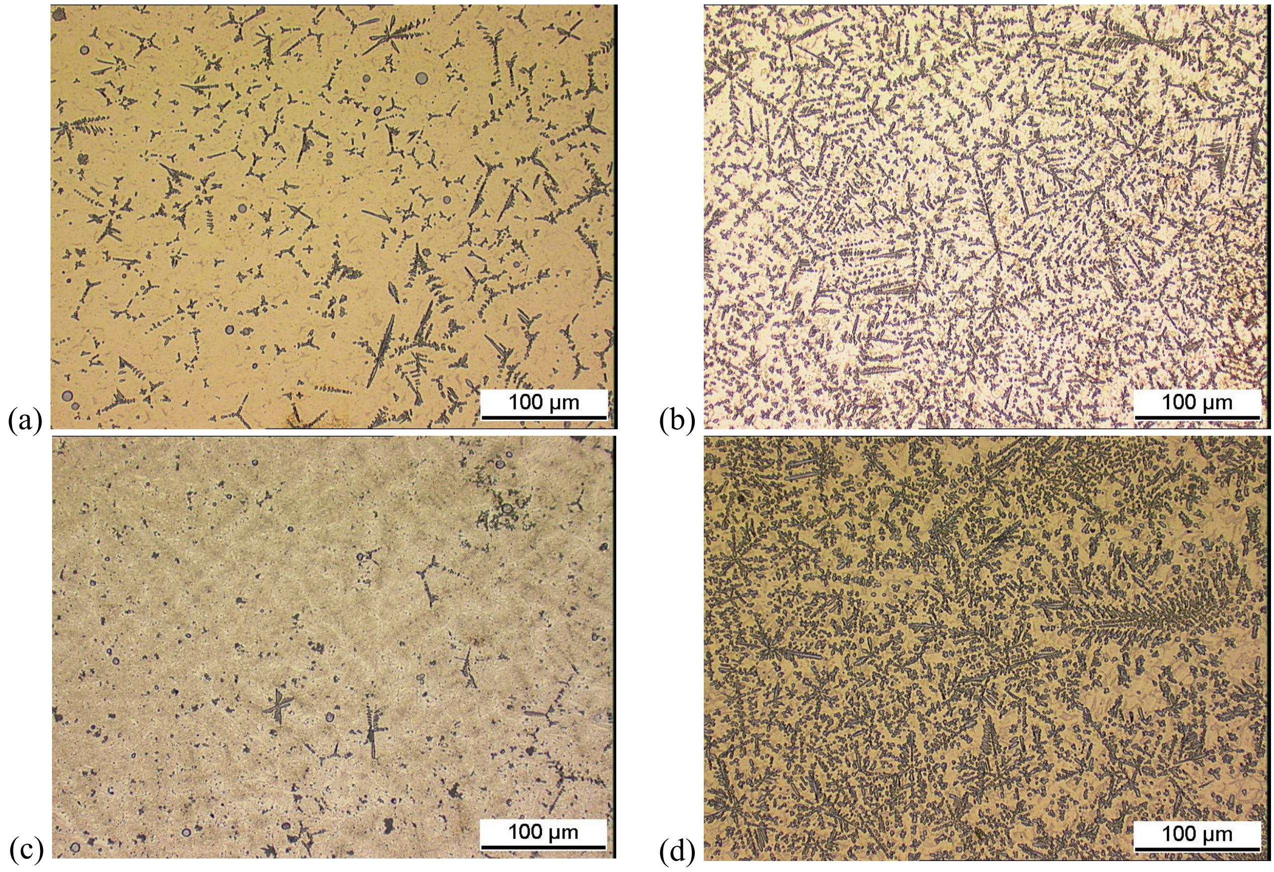

Fig. 7 : micrographs of MIG brazed joints obtained on DP600 with different filler wire (a) Nertalic46 CuAl8, (b) AlBz35 CuAlNi6, (c) Maxal 300 CuMn13Al7, (d) Mecufil 214Al.

2.2. VOLATILIZATION OF THE Zn LAYER

The Zn layer deterioration was investigated using a scanning electron microscope. The width of the Zinc depleted zone has been measured on the surface of the top and the bottom sheet and at back side. The results are shown in Table 5. A comparison is made between MAG welding, MIG braze welding and TIG braze welding of TRIP700 steel. For MAG welding, the parameters used were : 15.7V, 154 A and 35 cm/min with solid wire (Nertalic 70A) and ARCAL 21 shielding gas (Ar + 8% CO_2). The brazed specimens used for this comparison are those obtained with CuMn13Al7 filler wire.

Table 5 : Width of vaporization of the zinc layer on TRIP700 steel joint in MAG welding, MIG braze welding and TIG braze welding

Process Normalized heat input	**MAG welding** 1450 J/cm/mm	**MIG braze welding** 717 J/cm/mm	**TIG braze welding** 363 J/cm/mm
Top sheet	2 mm	0.9 mm	0.3 mm
Botton sheet	1.9 mm	0.9 mm	0.9 mm
Back side	5-6 mm	Small degradation of the Zn coating	No degradation of the Zn coating

These results clearly show the benefit of the lower heat input of MIG and TIG braze welding, leading to a reduction of the width of the Zn vaporization zone on the top sheet by 55% for MIG weld brazing and by 85% for TIG weld brazing compared to MAG welding. This table also shows that MIG and TIG braze welding avoid the deterioration of the Zn coating at back side. For MIG braze welding, there is no area for which the Zn layer is entirely vaporized, we can only notice a reduction of the Zn thickness at back side, whereas for MAG welding, the width of uncoated sheet is about 5 to 6 mm. This should lead to better corrosion resistance of the joints, in the case of MIG or TIG braze joints.

3. MECHANICAL RESULTS

Micro-hardness measurements (under 0.3 kg) in HAZ have been realized in order to assess the effect of heat input on the maximum hardness and width of the HAZ. Measurements were made on top sheet. A comparison has been made between MAG welding and MIG weld brazing on TRIP700 steel. For MAG welding, the parameters used were : 15.7V, 154 A and 35 cm/min with solid wire (Nertalic 70A) and ARCAL 21 shielding gas. The brazed specimen used is the one obtained with CuMn13Al7 filler wire. Fig. 8 shows the evolution of hardness HV0.3 along the Heat Affected Zone. The first point is measured at 30 µm from the fusion line in HAZ. A higher hardness in Coarse Grain Heat Affected Zone is observed for MIG braze welding, due to its lower heat input which leads to a high cooling rate. But this curve also shows that MIG braze welding allows to reduce the width of the Heat Affected Zone.

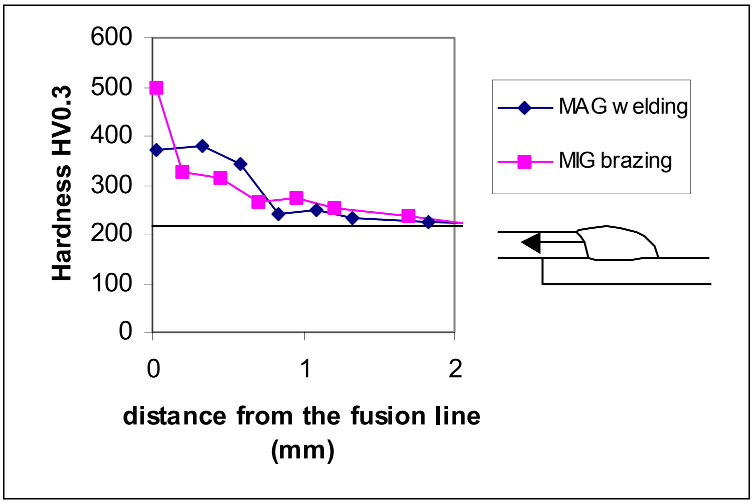

Fig. 8 : Hardness profile in Heat Affected Zone in TRIP700 steel

The results of mechanical tests are shown in Table 6. The results are expressed in terms of average joint efficiency . The joint efficiency is defined as the ratio between the tensile strength of the joint and the tensile strength of base metal. A joint efficiency of 100% means that the tensile strength of the joint at least equals the tensile strength of the base metal. We consider that results are satisfactory if the joint efficiency is above 85%. Values reported in the table are average values of the three tests realized. Table 6 also shows the localization of the failure for the three specimens.

MIG brazed joints on DP600 failed mainly in base metal. Even if some failures occur in weld metal, satisfactory joint efficiencies can be reached (95 – 100%). For TRIP700, only two filler wires allow to reach good joint efficiency (CuAl8 and flux cored wire). In the other cases, rupture always occurs in the weld metal. For TIG braze welding on DP600, the only joint characterized was realized with CuAl8 and lead to three ruptures in base metal. For TRIP700, CuAl8 gives good mechanical results, but rupture is located in weld metal. As in MIG braze welding, CuAlNi6 and CuMn13Al7 given lower results than CuAl8. Whereas, CuAlNi6 and CuMn13Al7 wires were chosen for their higher mechanical properties, the best results can be achieved with the standard wire CuAl8. The copper flux cored wire that was used in our evaluation showed no principal benefit in terms of mechanical resistance in static conditions.

Table 6 : Joint efficiency obtained in tensile-shear tests for MIG and TIG braze welding

Process	Filler wire	DP600		TRIP700	
		Joint efficiency	Rupture	Joint efficiency	rupture
MIG	CuAl8	100%	3 in BM	95%	2 in BM, 1 in WM
	CuAlNi6	95%	1 in BM, 2 in WM	60%	3 in WM
	CuMn13Al7	97%	2 in BM, 1 in WM	75%	3 in WM
	Mecufil 214Al	100%	3 in BM	90%	2 in BM, 1 in WM
TIG	CuAl8	100%	3 in BM	89%	3 in WM
	CuAlNi6			37%	3 in WM
	CuMn13Al7			44%	3 in WM

The ruptures occurring in weld metal were investigated by microscopic analyses. Fig. 9 shows that the rupture occurs in weld metal, near to the fusion line. In these cases, rupture initiates in the root of the joint and propagates either in the weld metal, either through the fusion line.

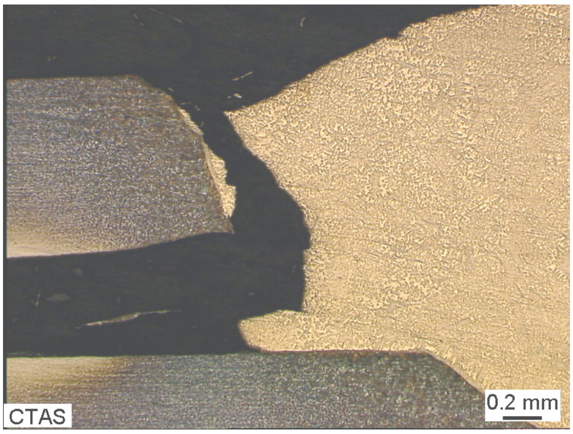

Fig. 9 : Localization of the rupture occurring in weld metal (here on DP600 brazed with CuMn13Al7).

The interface between base metal and copper bead has also been investigated. A very fine layer can be observed at the interface. The thickness of this layer is about 5 µm. The chemical composition of the layer was investigated using SEM and EDX analysis, as shown in Fig. 10. The interface layer is mainly composed of iron, copper and other alloying elements present in the filler wire (Al, Mn). The presence of this interface layer, which may be hard, can embrittle the joint. Fig. 10 also shows that dendrites grow in the copper matrix starting on this interface layer.

(a) 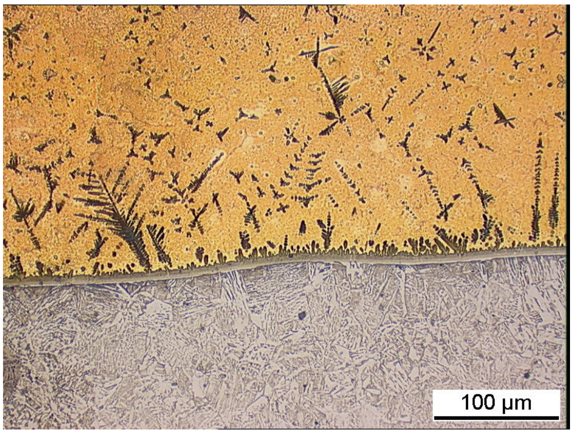

(b) 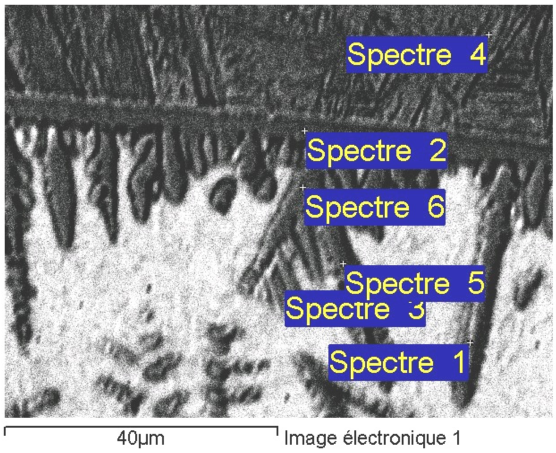

(c)

Spectre	Al	Si	Cr	Mn	Fe	Ni	Cu
Spectre 3 (copper matrix)	8.0			12.1	4.7	2.3	72.8
Spectre 1 (dendrite)	7.5	0.3		13.3	30.5	2.5	46.0
Spectre 5 (dendrite)	7.4	0.3	0.2	12.3	60.5	2.7	16.7
Spectre 6 (dendrite)	8.2			11.8	54.6	2.3	23.0
Spectre 2 (interface layer)	5.9	0.2	0.3	8.6	71.8	1.6	11.7
Spectre 4 (base metal)	1.3		0.4	1.5	96.2		0.6

Fig. 10 : Investigations of the interface layer for MIG weld brazing of DP600 with CuMn13Al7 filler wire (a) micrograph, (b) SEM image and (c) EDX chemical analysis of areas in (b) .

4. CONCLUSIONS

In the experimental work in CTAS a representative, but yet not exhaustive choice of steel grades and filler wires has been tested to assess their compatibility following the car manufacturers specifications. All the joints realized were characterized by tensile-shear testing and macro and micrographic examination.

From a mechanical point of view, all the results with DP600 steel were good. For TRIP700 steel, joint efficiencies are lower due to higher tensile strength of the base metal. Nevertheless, CuAl8 leads to satisfactory results.

From an operating point of view, MIG and TIG weld brazing seemed to be very promising because it should supply more reliable welding operation than welding on thin steel gauge. The results obtained with TIG weld brazing are similar to those with MIG weld brazing. Obviously, TIG weld brazing permits to realize beads without any spatters compared to MIG weld brazing.

This study shows that the low heat input of braze welding processes helps to reduce the width of the heat affected zone in the base metal and limits the Zn coating degradation besides the bead and back side.

REFERENCES

1) G. WEBER and S. GÖKLU, “Resistance Spot Welding of Advanced High-Strength Steels, influence of welding parameters and electrode cap”, Proceedings of IIW International Conference, Prague (2005).
2) Use of ULSAB technologies by automakers growing rapidly, AISI Press Release (2000).
3) ULSAB-AVC – PES Engineering Report, Materials and Processes (2001).

4) T. SENUMA, “Physical Metallurgy of modern high strength steel sheets”, ISIJ International, vol. 41 n°6, (2001), p. 520-532.
5) Technical specification PSA (confidential)
6) Technical Specifications Renault (confidential)
7) T. OPDERBECKE and S. GUIHEUX, „TOPTIG: WIG Roboterschweißen mit Kaltdrahtzufuhr bringt Schweißqualität und Geschwindigkeit“, DVS Proceedings, „Schweissen und schneiden 2005“, Essen (2005).
8) DVS Merkblatt « Lichtbogenloeten Teil 1 und 2 »